Our direct calculation of a resonance energy includes the effort of a full ab initio SCF calculation of the molecule considered. One could, of course, use the SCF energy itself for drawing conclusions about the stability of the molecule. In addition, one could compute theoretically the enthalpy changes of isodesmic and of homodesmotic reactions in order to deduce resonance energies defined in the same way as the experimental resonance energies. This would, however, still not answer the conceptually interesting question: which part of the stability of a molecule can be attributed to the resonance in the π system? Moreover, resonance energies directly calculated from model wave functions are expected to depend less on the basis set and less on the details of the structural parameters, like valence angles and CH bond lengths, than the total SCF energy. Since larger π systems can only be calculated within minimal basis sets, the total SCF energy has not much meaning and is certainly less accurate than a directly computed resonance energy.

The principle of calculating an energy expectation value with respect to a model wave function can as well be applied to other terms used in chemistry which are based on certain models, like hyperconjugation, inductive effects, etc. In the analysis of molecular interactions (hydrogen bonds, certain regions of a potential energy surface of a chemical reaction) reference states containing the molecular orbitals of unperturbed subsystems could be of some interest.

Acknowledgment. The calculations were performed partly on a Telefunken TR 440 computer of the computation center of the university and partly on an Interdata 8/32 minicomputer which was granted to our group by the Deutsche Forschungsgemeinschaft.

References and Notes

(1) E. Hückel, *Z. Elektrochem.*, **43**, 752, 827 (1937).
(2) G. W. Wheland, "Resonance in Organic Chemistry", Wiley, New York, 1955.
(3) A. Streitwieser, "Molecular Orbital Theory for Organic Chemists", Wiley, New York, 1961.
(4) L. Salem, "The Molecular Orbital Theory of Conjugated Systems", W. A. Benjamin, New York, 1966.
(5) R. S. Mulliken and R. G. Parr, *J. Chem. Phys.*, **19**, 1271 (1951).
(6) M. J. S. Dewar, "The Molecular Orbital Theory of Organic Chemistry", McGraw-Hill, New York, 1969.
(7) (a) M. J. S. Dewar and G. J. Gleicher, *J. Am. Chem. Soc.*, **87**, 692 (1965); (b) *Tetrahedron*, **21**, 3423 (1965); (c) A. L. H. Chung and M. J. S. Dewar, *J. Chem. Phys.*, **42**, 756 (1965); (d) M. J. S. Dewar and C. deLlano, *J. Am. Chem. Soc.*, **91**, 789 (1969); (e) M. J. S. Dewar and A. J. Harget, *Proc. R. Soc. London, Ser. A*, **315**, 443 (1970).
(8) P. George. *Chem. Rev.*, **75**, 85 (1975).
(9) (a) P. George, M. Trachtman, C. W. Bock, and A. M. Brett, *J. Chem. Soc., Perkin Trans. 2*, 1222 (1976); (b) *Tetrahedron*, **32**, 1357 (1976).
(10) L. A. Carreira, *J. Chem. Phys.*, **62**, 3851 (1975).
(11) R. Pariser and R. G. Parr, *J. Chem. Phys.*, **21**, 466 (1953); J. A. Pople, *Trans. Faraday Soc.*, **49**, 1375 (1953).
(12) D. H. Lo and M. A. Whitehead, *Can. J. Chem.*, **46**, 2027, 2041 (1968).
(13) J. Kao and N. L. Allinger, *J. Am. Chem. Soc.*, **99**, 975 (1977).
(14) B. A. Hess, Jr., L. J. Schaad, and I. Agranat, *J. Am. Chem. Soc.*, **100**, 5268 (1978); B. A. Hess, Jr., and L. J. Schaad, *ibid.*, **94**, 3068 (1972); **93**, 305 (1971).
(15) (a) J. P. Figeys, *Tetrahedron*, **26**, 4615, 5225 (1970); (b) J. Aihara, *J. Am. Chem. Soc.*, **99**, 2048 (1977); (c) W. C. Herndon and M. L. Ellzey, Jr., *ibid.*, **96**, 6631 (1974); (d) I. Gutman, M. Milun, and N. Trinajstic, *ibid.*, **99**, 1692 (1977).
(16) M. J. S. Dewar, *Pure Appl. Chem.*, **44**, 767 (1975).
(17) W. H. Hehre, R. Ditchfield, L. Radom, and J. A. Pople, *J. Am. Chem. Soc.*, **92**, 4796 (1970).
(18) M. H. Palmer and R. H. Findlay, *J. Chem. Soc., Perkin Trans. 2*, 1985, 1993 (1974).
(19) S. F. Boys, *Rev. Mod. Phys.*, **32**, 296 (1960).
(20) R. Ahlrichs, *Theor. Chim. Acta*, **33**, 157 (1974).
(21) H. Kollmar, unpublished.
(22) S. Huzinaga, *J. Chem. Phys.* **42**, 1293 (1965); "Approximate Atomic Functions I", IBM Publication, 1971.
(23) W. Meyer, *J. Chem. Phys.*, **58**, 1017 (1973); *Int. J. Quantum Chem., Symp.*, **5**, 59 (1971).
(24) R. Ahlrichs, H. Lischka, V. Staemmler, and W. Kutzelnigg, *J. Chem. Phys.*, **62**, 1225 (1975).
(25) R. J. Buenker and S. D. Peyerimhoff, *Chem. Phys.*, **9**, 75 (1975); V. Staemmler, *Theor. Chim. Acta*, **45**, 89 (1977).
(26) W. J. Hehre and J. A. Pople, *J. Am. Chem. Soc.*, **97**, 6941 (1975).
(27) A. Bander and H. H. Günthard, *Helv. Chim. Acta*, **45**, 1698 (1962).
(28) A. L. McClellan, "Tables of Experimental Dipole Moments", W. H. Freeman, San Francisco, 1963.
(29) K. Hafner, *Angew. Chem., Int. Ed. Engl.*, **3**, 165 (1964).
(30) H. Kwoda, T. Ohta, and T. L. Kunii, *Jerusalem Symp. Quantum Chem. Biochem.*, **3** (1971).
(31) H. J. Tobler, A. Bander, and H. H. Günthard, *J. Mol. Spectrosc.*, **18**, 239 (1965); J. M. Robertson, M. M. Schaerer, G. A. Sim, and D. G. Watson, *Acta Crystallogr.*, **15**, 1 (1962); A. W. Hansen, **19**, 19 (1965); O. Bastiansen and J. L. Derisson, *Acta Chem. Scand.*, **20**, 1319 (1966).
(32) R. C. Bingham, M. J. S. Dewar, and D. H. Lo, *J. Am. Chem. Soc.*, **97**, 1285 (1975).
(33) R. J. Buenker and S. D. Peyerimhoff, *Chem. Phys. Lett.*, **3**, 37 (1969).
(34) S. Becker, D. Heidrich, and C. Weiss, *Z. Chem.*, **14**, 440 (1974).
(35) G. Binsch and I. Tamir, *J. Am. Chem. Soc.*, **91**, 2450 (1969).
(36) J. H. Callomon and B. P. Stoichaff, *Can. J. Phys.*, **35**, 373 (1957).

In Situ Resonance Raman Spectroscopic Investigation of the Tetrathiafulvalene–Tetracyanoquinodimethane Electrode Surface

William L. Wallace, Calvin D. Jaeger, and Allen J. Bard*

Contribution from the Department of Chemistry, The University of Texas at Austin, Austin, Texas 78712. *Received October 16, 1978*

Abstract: Resonance Raman spectroscopy was applied to the study of the tetrathiafulvalene-tetracyanoquinodimethane (TTF-TCNQ) electrode in an aqueous 1.0 M KBr solution and spectroscopic evidence is presented which shows that oxidative decomposition of the electrode results in the formation of neutral TCNQ. Subsequent waves for surface processes in the cyclic voltammetry of the oxidized TTF-TCNQ electrode can be directly attributed to the reduction of electrogenerated TCNQ and reoxidation of the reduced product (KTCNQ) by simultaneously monitoring the current and the Raman intensity of the strongest neutral TCNQ band as a function of applied potential.

The in situ characterization of heterogeneous electron transfer reactions occurring at the electrode-solution interface by the techniques of normal and resonance Raman spectroscopy has been shown to be feasible and highly informative. To date several studies have been reported characterizing (1) stable electrogenerated species produced by exhaustive electrolysis and monitored under steady-state conditions in the bulk solution;[1] (2) transient species generated in the electrochemical diffusion layer;[2] (3) species undergoing potential-controlled adsorption on metal and semiconductor electrodes;[3,4] (4)

0002-7863/79/1501-4840$01.00/0

species generated on the electrode surface as a result of primary homogeneous solid state electron transfer reactions of the electrode itself (electrode decomposition).[5] In this communication resonance Raman data is reported which identifies unequivocally and in a molecularly specific manner some of the reactions which occur as a result of the electrochemical decomposition of the TTF-TCNQ electrode.[6a] A detailed electrochemical investigation of this electrode in several electrolytes has recently been reported;[6b] here we concentrate on the oxidation of the TTF-TCNQ electrode in a 1.0 M KBr aqueous solution.

Electrochemical measurements were made using a two-compartment Pyrex cell fitted with Pyrex optical windows on the bottom and one side of the 25-mL working electrode compartment. Potentiostatic control and measurements were made using equipment and techniques previously described.[6b] Electrochemical potentials were measured with respect to the $Ag/AgNO_3$ (0.01 M) reference electrode which was isolated in a Teflon tube fitted with a porous Vycor glass frit. Raman measurements were made using a Cary Model 82 Raman spectrophotometer fitted with Model 164 Ar and Kr ion lasers. The electrochemical cell described above was used as the Raman cell employing an oblique scattering geometry similar to configurations previously described.[3b,d,5b] Raman frequencies were calibrated using the discrete line output of a Ne lamp.[7]

The electrochemical behavior of the TTF-TCNQ electrode in a 1.0 M KBr solution is depicted in the first scan and steady-state cyclic voltammograms in Figure 1. Also shown in this figure is the electrochemical behavior, in 1.0 M KBr, of TTF deposited on Pt by evaporation from a benzene solution. Prior to lattice oxidation at +0.53 V the TTF-TCNQ electrode exhibits a stable potential region (+0.53 to −0.22 V) characterized by the presence of small residual background currents. However, five clearly distinguishable surface waves, three cathodic (A, +0.51 V; B, +0.12 V; C, + 0.01 V) and two anodic (D, +0.19 V; E, +0.35 V) (steady-state peak potentials vs. $Ag/AgNO_3$ (0.01 M)), are observed in this stable potential region after the passage of anodic current at potentials positive of +0.53 V. Small potential shifts are observed upon repetitive scanning between +0.45 and −0.01 V approaching the limiting potentials observed in the steady-state cyclic voltammogram. The data in Figure 1 are derived from two different TTF-TCNQ electrodes (different areas and total charge passed for lattice oxidation) and are representative of variations in relative peak height ratios, peak widths, and potential differences observed for several electrodes. By scanning in the negative direction from approximately +0.50 V and reversing the scan at successively more negative potentials it can be shown that anodic peaks E and D appear only after reduction processes B and C have occurred, respectively, thus showing a coupling in the electrochemistry for processes B/E and C/D.

Evidence generated from studies involving the variation in electrochemical behavior of the TTF-TCNQ electrode as a function of supporting electrolyte, the electrochemical behavior of TTF- and TCNQ-impregnated compressed polycrystalline graphite electrodes, and the electrochemistry of Pt electrodes coated with thin films of TTF and TCNQ indicates that the various redox processes occurring in Figure 1 can be attributed to the following reactions:[6b]

$$\text{(B) } TCNQ + K^+ + e^- \rightarrow KTCNQ \quad (1)$$

$$\text{(C) } TTFBr + e^- \rightarrow TTF + Br^- \quad (2)$$

$$\text{(D) } TTF + Br^- \rightarrow TTFBr + e^- \quad (3)$$

$$\text{(E) } KTCNQ \rightarrow TCNQ + K^+ + e^- \quad (4)$$

The presence of all four compounds listed in eq 1-4 as solids on the electrode surface at various potentials has been confirmed by infrared spectroscopy.[8] The primary lattice oxidation process appears to involve the transfer of two electrons per TTF-TCNQ moiety forming neutral TCNQ and TTF^{2+} (eq 5) and peak A can be attributed to the reduction of TTF^{2+} to form TTFBr (eq 6).[6b]

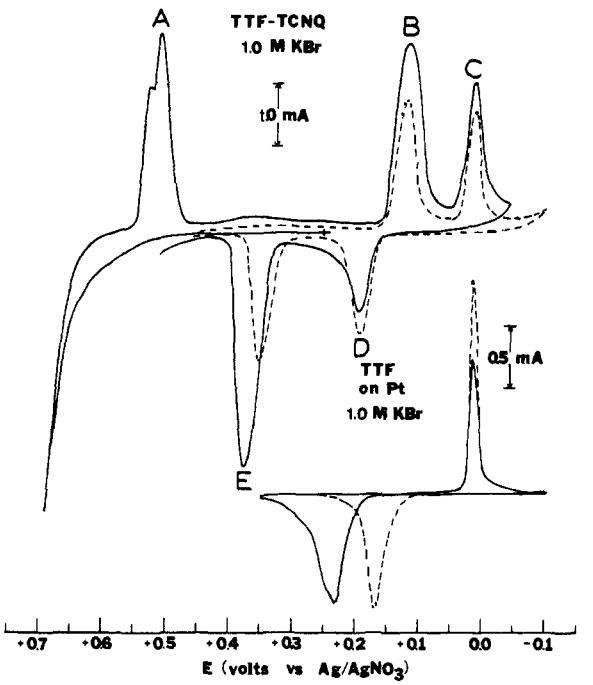

Figure 1. Top: first scan (—) and steady-state (---) cyclic voltammograms of the TTF-TCNQ electrode. Bottom: first scan (—) and steady-state (---) cyclic voltammograms of TTF on Pt. Scan rate, 20 mV s^{-1}; aqueous 1.0 M KBr; potentials vs. the $Ag/AgNO_3$ (0.01 M) reference electrode.

$$TTF\text{-}TCNQ \rightarrow TTF^{2+} + TCNQ + 2e^- \quad (5)$$

$$TTF^{2+} + Br^- + e^- \rightarrow TTFBr \quad (6)$$

The insert showing the first scan and steady-state cyclic voltammetric behavior of TTF on Pt in Figure 1 reveals the very similar electrochemical behavior (peak shapes, approximate peak ratios, and relative peak widths) of TTF on the two different electrode surfaces in the same supporting electrolyte-solvent system. In general the variation in peak potential of the anodic wave (eq 3) in successive scans was not as large on the TTF-TCNQ electrode as on Pt.

Spectroscopic evidence for the formation of TCNQ on the surface of the TTF-TCNQ electrode is also provided by the Raman spectrum shown in Figure 2. In terms of vibrational frequencies and relative peak intensity ratios this spectrum can be unequivocally identified as that of neutral TCNQ by comparison with literature spectra.[1c] Eight out of ten of the totally symmetric (A_g) modes of TCNQ (D_{2h} symmetry) are evident and there are no significant frequency shifts. The spectrum can be designated as resonance enhanced by virtue of the proximity of the exciting line (4880 Å) to the lowest energy absorption band of solid TCNQ[9] and the appearance of totally symmetric modes only.[1c]

Initially no Raman bands could be detected with a fresh TTF-TCNQ electrode in the electrochemical-Raman cell immersed in 1.0 M KBr aqueous solution with laser excitation wavelengths varying from 4579 to 6457 Å at powers ranging from 10 to 50 mW at the cell window and at applied potentials in the stable potential region described above. The spectrum in Figure 2 was obtained only after lattice oxidation which in turn could be detected by monitoring the intensity of the strongest Raman band at 1454 cm^{-1} as a function of applied

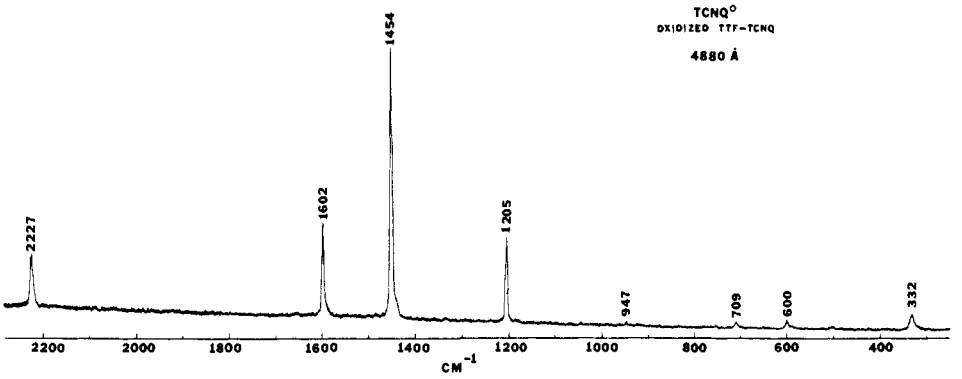

Figure 2. Resonance Raman spectrum of $TCNQ^0$ on the surface of TTF-TCNQ (1.0 M KBr aqueous solution) with cell in open circuit condition after lattice oxidation at +0.65 V vs. $Ag/AgNO_3$ (0.01 M). Scan rate, 1.0 cm^{-1} s^{-1}; bandwidth, 2.0 cm^{-1}.

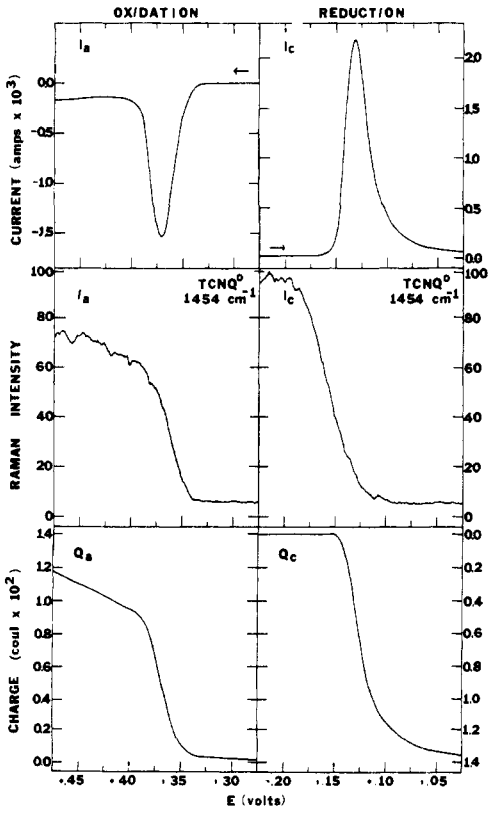

Figure 3. Current (top), Raman intensity (middle), and charge (bottom) recorded simultaneously as a function of applied potential for the oxidation of KTCNQ (left) and reduction of $TCNQ^0$ (right) on the TTF-TCNQ electrode (area, 0.065 cm^2) in aqueous 1.0 M KBr. Scan rate, 5 mV s^{-1}; direction of scan indicated by arrows; Raman intensity monitored at 1454 cm^{-1}; bandwidth, 3.0 cm^{-1}; Raman recorder pen RC time constant, 1.0 s; excitation wavelength, 4880 Å.

potential. For example, upon initiating a potential scan in the positive direction an increase in Raman intensity, initially at the background scattering level, is observed at the potential corresponding to the onset of anodic current for lattice oxidation. This result provides confirmatory evidence that lattice oxidation promotes the formation of $TCNQ^0$ (eq 5). Oxidation of TTF-TCNQ also results in a color change of the electrode surface from dark green (almost black) to yellow. Prolonged oxidation of the electrode leads to a saturation in Raman intensity implying the formation of a film of TCNQ on the electrode surface with a thickness greater than the penetration depth of the excitation radiation. With excitation wavelengths $\geq$4880 Å ($\leq$40 mW at cell window) the Raman intensity at 1454 cm^{-1} was constant as a function of time and applied potential between $\sim$+0.45 and $\sim$+0.18 V and did not change when the cell was placed at open circuit. A noticeable decrease in Raman intensity with time was observed with an excitation wavelength of 4658 Å (10-mW laser power at the cell window). This disappearance of TCNQ is attributed to a photochemical or thermal reaction induced by light absorption in the low molar absorptivity tail of the low-energy solid TCNQ absorption band. Under the conditions of cell design and scattered light collection geometry employed, $TCNQ^0$ was the only compound which could be detected on the oxidized electrode surface by Raman spectroscopy at applied potentials between +0.5 and −0.1 V and with excitation wavelengths between 4579 and 6457 Å at laser powers varying between 10 and 100 mW at the cell window.

The relationship between current, relative Raman intensity, charge, and potential is shown in Figure 3 for the TCNQ/KTCNQ couple at +0.12 and +0.35 V. The three profiles for current, Raman intensity, and charge monitored as a function of potential were recorded simultaneously for one sample and are representative of results obtained from three different electrodes. The current-potential curves in Figure 3 were reproducible and deviated by less than 10% in peak height and charge for five successive scans. Several basic features immediately evident in the figure upon examination can be summarized in the following observations. The Raman intensity of $TCNQ^0$ (1454-cm^{-1} band) decreases to the background scattering level at potentials corresponding to the cathodic wave previously attributed to the reduction of TCNQ from electrochemical studies (eq 1). The TCNQ Raman signal is regenerated (generally to within 80-90% of the prereduction value) at potentials corresponding to the anodic wave previously attributed to the oxidation of KTCNQ (eq 4). Finally, the Raman intensity-potential profiles in both cases have approximately the same shape (potential dependence) as the corresponding charge-potential profiles.[10] These results including the observed intensity and charge-potential profiles are reminiscent of results previously obtained for (1) absorption and Raman spectroscopic studies using thin layer cells,[2b,11] in which heterogeneous electron transfer reactions exhibit electrochemical characteristics similar to adsorption behavior; (2) Raman studies of various species adsorbed on semiconductor electrodes;[4] (3) Raman studies of oxide formation on various metal electrodes.[5] The Raman results taken together with the electrochemical results[6] provide conclusive evidence that the cathodic and anodic waves pictured in Figure 3 (waves B and E, respectively, in Figure 1) can be attributed to the reduction and oxidation of TCNQ and its reduced form (KTCNQ), respectively. In addition the data in this communication further demonstrates the potential power of Raman spectroscopy coupled with electrochemistry under favorable conditions in deciphering the details of heterogeneous redox reactions occurring at an electrode surface.

References and Notes

(1) (a) Suchanski, M. R.; Van Duyne, R. P. *J. Am. Chem. Soc.* **1976**, *98*, 250. (b) Jeanmaire, D. L.; Suchanski, M. R.; Van Duyne, R. P. *Ibid.* **1975**, *97*, 1699. (c) Jeanmaire, D. L.; Van Duyne, R. P. *Ibid.* **1976**, *98*, 4029. (d) *Ibid.* **1976**, *98*, 4034.

(2) (a) Jeanmaire, D. L.; Van Duyne, R. P. *J. Electroanal. Chem.* **1975**, *66*, 235. (b) Clarke, J. S.; Kuhn, A. T.; Orville-Thomas, W. J. *Ibid.* **1974**, *54*, 253.

(3) (a) McQuillan, A. J.; Hendra, P. J.; Fleischmann, M. *J. Electroanal. Chem.* **1975**, *65*, 933. (b) Cooney, R. P.; Fleischmann, M.; Hendra, P. J. *J. Chem. Soc., Chem. Commun.* **1977**, 235. (c) Paul, R. L.; McQuillan, A. J.; Hendra, P. J.; Fleischmann, M. *J. Electroanal. Chem.* **1975**, *66*, 248. (d) Fleischmann, M.; Hendra, P. J.; McQuillan, A. J. *Chem. Phys. Lett.* **1974**, *26*, 163. (e) Albrecht, M. G.; Creighton, J. A. *J. Am. Chem. Soc.* **1977**, *99*, 5215. (f) Cooney, R. P.; Reid, E. S.; Hendra, P. J.; Fleischmann, M. *ibid.* **1977**, *99*, 2002. (g) Cooney, R. P.; Hendra, P. J.; Fleischmann, M. *J. Raman Spectrosc.* **1977**, *6*, 264. (h) Jeanmaire, D. L., Van Duyne, R. P. *J. Electroanal. Chem.* **1977**, *84*, 1. (i) Pettinger, B.; Wenning, U. *Chem. Phys. Lett.* **1978**, *56*, 253. (j) Creighton, J. A.; Albrecht, M. G.; Hester, R. E.; Matthew, J. A. D. *Ibid.* **1978**, *55*, 55.

(4) (a) Yamada, H.; Amamiya, T.; Tsubomura, H. *Chem. Phys. Lett.* **1978**, 56, 591. (b) Fujihira, M.; Osa, T. *J. Am. Chem. Soc.* **1976**, *98*, 7850.

(5) (a) Fleischmann, M.; Hendra, P. J.; McQuillan, A. J. *J. Chem. Soc., Chem. Commun.* **1973**, 80. (b) Fleischmann, M.; Hendra, P. J.; McQuillan, A. J.; Paul, R. L.; Reid, E. S. *J. Raman Spectrosc.* **1976**, *4*, 269. (c) Reid, E. S.; Hendra, P. J.; Fleischmann, M. *J. Electroanal. Chem.* **1977**, *80*, 405.

(6) (a) The tetrathiafulvalene (TTF)–tetracyanoquinodimethane (TCNQ) electrodes were in the form of highly conducting pellets prepared by compressing polycrystalline TTF–TCNQ. (b) Jaeger, C. D.; Bard, A. J. *J. Am. Chem. Soc.*, **1979**, *101*, 1690.

(7) Robinson, J. W., Ed. "Handbook of Spectroscopy", Vol. II; CRC Press: Cleveland, 1974.

(8) Infrared spectra were obtained using a Beckman IR-9 infrared spectrophotometer by scraping electrogenerated material off the electrode surface, carefully avoiding contamination by bulk TTF–TCNQ. Samples were prepared as pressed KBr pellets. The infrared spectrum of material produced by scanning to −0.1 V after initially oxidizing the electrode at +0.75 to +0.80 V clearly revealed the presence of TTF^0 and KTCNQ by comparison with spectra of the pure compounds. If the potential was scanned to −0.1 V, then reversed and scanned back to +0.5 V, infrared spectra clearly showed the presence of TTFBr and $TCNQ^0$. Further details will be published in the Ph.D. dissertation of C.D.J.

(9) (a) Hiroma, S.; Kuroda, H.; Akamatu, H. *Bull. Chem. Soc. Jpn.* **1970**, *43*, 3626. (b) Eckhardt, C. J.; Pennelly, R. R. *Chem. Phys. Lett.* **1971**, *9*, 572.

(10) For heavily oxidized TTF–TCNQ electrodes (as many as 5000 monolayers consumed using the criteria in ref 6) the Raman intensity decreased by 90% before passage of ≤50% of the total charge for TCNQ reduction (Figure 3), possibly indicating that the most Raman-active surface layers are reduced significantly before the Raman-inactive subsurface layers. Further study of this unusual behavior by a careful examination of the Raman intensity–potential profiles as a function of surface coverage could not be accomplished in this investigation because of the sensitivity limitations at low coverages.

(11) (a) Murray, R. W.; Heineman, W. R.; O'Dom, G. W. *Anal. Chem.* **1967**, *39*, 1666. (b) Kuwana, T.; Heineman, W. R. *Acc. Chem. Res.* **1976**, *9*, 241, and references cited therein.

(12) The support of this research by the National Science Foundation and the Robert A. Welch Foundation is gratefully acknowledged. We also thank Professor William H. Woodruff for his assistance in these studies.

Molecular Orbital Theory of the Electronic Structure of Molecules. 39. Highly Unusual Structures of Electron-Deficient Carbon Compounds. Reversal of van't Hoff Stereochemistry in BBC Ring Systems[1]

K. Krogh-Jespersen,[2a,b] D. Cremer,[2c] D. Poppinger,[2a,d] J. A. Pople,[2e] P. v. R. Schleyer,*[2a] and J. Chandrasekhar[2a]

Contribution from the Institut für Organische Chemie der Universität Erlangen-Nürnberg, 8520 Erlangen, Federal Republic of Germany, the Lehrstuhl für Theoretische Chemie der Universität Köln, 5000 Köln, Federal Republic of Germany, and the Department of Chemistry, Carnegie-Mellon University, Pittsburgh, Pennsylvania 15213.
Received January 2, 1979

Abstract: It may be possible to violate all of van't Hoff's stereochemical rules! When two geminal hydrogens of methane, of ethylene, of allene, or of butatriene are replaced by a three-membered ring comprised of two BH groups, ab initio molecular orbital calculations indicate preference for anti-van't Hoff geometries: planar $(HB)_2CH_2$ (**6b**), perpendicular $(HB)_2C{=}CH_2$ (**7b**), planar $(HB)_2C{=}C{=}CH_2$ (**8b**), and perpendicular $(HB)_2C{=}C{=}C{=}CH_2$ (**9b**). These forms are estimated to be 15–20 kcal/mol more stable than the van't Hoff alternatives, **6a–9a**. The van't Hoff forms (**6a–9a**) exhibit classical Lewis two-center–two-electron bonding, with six σ electrons for the three diboracyclopropane ring bonds. In the anti-van't Hoff forms (**6b–9b**), the same rings have only four σ electrons; the two remaining electrons occupy an aromatic, cyclopropenium-ion-like π orbital. The geometrical consequences are shortening of the BB bonds and widening of the HBB angles in **6b–9b** over **6a–9a**, and, most particularly, retention of the exocyclic $C_1{=}C_2$ double bonds in the anti-van't Hoff forms (**7b–9b**). Both the perpendicular ethylene **7b** and its less stable planar isomer **7a** are found to be local minima, with a rotation barrier between them. Triplet forms of **6–9** do not appear to be competitive in energy with the singlets. Prospects for the experimental verification of these predictions are analyzed. Isolobal transition metal analogues may be best suited for this purpose.

Introduction

By linking carbon-based tetrahedra edge to edge, van't Hoff deduced in 1875 that the basic shapes of the cumulenes (**1**) should vary periodically.[3] When the number of double bonds, n, is odd, planarity (D_{2h} symmetry) is preferred, but perpendicular arrangements (D_{2d}) are favored when n is even. Methane (T_d), **1** with $n = 0$, can be considered to be the first member of this perpendicular series. These were remarkable predictions! At the time, neither allene (**1**, $n = 2$) nor any of its derivatives were known, and 60 years passed before van't Hoff's speculations concerning its stereochemistry were verified.[4] With butatriene (**1**, $n = 3$), an additional 24 years were required,[5] and the ground-state geometry of a pentatetraene was first established experimentally in 1976.[6] The rotational barrier in ethylene (**1**, $n = 1$) (65 kcal/mol) was determined in 1955,[7] but those for allene (~48 kcal/mol),[8] butatriene (~34 kcal/mol),[9,10] and the higher cumulenes only are of recent date.[10]

$$H_2C(=C)_nH_2$$
1

0002-7863/79/1501-4843$01.00/0